Compact tunable monolithic sensors for vibration monitoring and control of structures and very low frequency – large band characterization of sites

F. Acernese, G. Giordano, R. Romano & F. Barone
University of Salerno, Italy and INFN, Sez. Napoli, Italy

SUMMARY
In this paper we describe a new mechanical implementation of a horizontal monolithic folded pendulum inertial sensor, configurable as low-frequency large-band seismometer and/or accelerometer, for seismic monitoring (strong motion and seismic noise characterization) and for monitoring and control of scientific, civil and industrial structures, also in difficult environmental conditions (mines, dangerous conditions, high vacuum, low temperature and cryogenic environment). The very large measurement band ($10^{-7} \div 10\ Hz$), low readout noise $< 10^{-8}\ m/\sqrt{Hz}$ in the band $(0.01\ \div 10\ Hz)$ with laser optical lever readout and $< 10^{-12}\ m/\sqrt{Hz}$ in the band $(0.01\ \div 10\ Hz)$ with laser interferometric readout) are its main characteristics. Moreover, scalability, compactness $(l\ < 15\ cm)$, light weight $(< 2\ Kg)$, tunability down to $\approx 66\ mHz$ and high quality factor $(> 1500$ in air) are other very relevant features. In the paper, after a general description of the seismometer, we present and discuss preliminary scientific data recorded in the INFN Gran Sasso National Laboratory (LNGS).

Keywords: Seismometer, Accelerometer, Folded Pendulum, Monolithic Sensor, Seismic Monitoring

1. INTRODUCTION

The output signal of a classic seismometer is proportional to the displacement (or velocity) of the test mass due to the inertial force generated by seismic ground motion. This technique is used today only in short-period seismometers. In fact, broadband seismometers generally use a force feed-back design, which largely improves linearity and dynamic range of the sensor. In these instruments a feedback force, generated with suitable control systems and applied to the test mass through an electromagnetic transducer, compensates the inertial force. The feedback force is then proportional to the ground acceleration, such as the current used to drive the transducer. Therefore, although technology has largely improved in these years, all the new designs of seismic sensors based on a force feed-back configuration have to face the limitations to their sensitivity and band due to the electronic noise of the force feed-back controls and of the readout systems.

The Folded Pendulum (hereafter FP) scheme, called also *Watt-linkage*, a classical suspension system developed in 1962 (Fergusson, 1962), seems to be the right key to solve some of these problems. In fact, its basic architecture was already used for the development of very effective vibration isolation system for gravitational wave detectors (Liu, Li and Blair, 1997) and in low frequency accelerometric sensors (Liu, Blair and Li, 2004; Zhou, Yi, Wu and Luo, 2004). Moreover, compact monolithic tunable sensors of small size with extremely soft flexures at the pendulum's hinges were implemented (Bertolini, et al., 2006; Bertolini, DeSalvo, Fidecaro, Takamori, 2006; Acernese, et al., 2008), whose sensitivity and immunity to environmental noise has been largely improved with the introduction of laser optics readout techniques (Acernese, et al., 2008, Acernese, et al., 2010a; Acernese, et al., 2010b). Moreover, special tuning procedures have been also developed to decrease the sensor natural resonance frequency (down to values of $\approx 66\ mHz$) (Acernese, et al., 2011), enlarging the measurement band, and consequently its sensitivity, in the low frequency region of the seismic spectrum. These results open new applications for this class of sensors, like, for example, geophysical applications aimed to explore the low frequency band of the seismic spectrum, both as a stand-alone sensor or as part of large and geographically distributed seismic networks.

Following this way, we developed a low-noise high-resolution horizontal monolithic FP sensor (UNISA Horizontal Seismometer) (Barone and Giordano, 2011), that can be configured as accelerometer (force feed-back configuration), but, and this is the one of its most interesting features, as low frequency high sensitivity large dynamics seismometer (no force feed-back). Interesting applications of this monolithic sensor already exist both as seismometer (Acernese, et al., 2012a) and as sensor in the control of seismic attenuators and inertial platforms (Acernese, et al., 2012b).

In the following sections we will describe the UNISA Horizontal Seismometer, discussing its mechanical performances and sensitivity in connection with different optical readout configurations. Finally, we present some results of its application as seismometer in the INFN Gran Sasso National Laboratory (LNGS).

2. THE THEORETICAL MODEL

A FP can be modelled according to the mechanical scheme shown in Fig. 2.1, with two vertical beams of equal length, l, a pendulum of mass m_{p_1} and an inverted pendulum of mass m_{p_2}, concentrated in their centers of mass in P_1 and P_2, respectively, at $l_b = l/2$. The central mass, m_C, is modeled, instead, with two equivalent masses, m_{C_1} and m_{C_2} ($m_C = m_{C_1} + m_{C_2}$), concentrated in the pivot points C_1 and C_2, respectively at the same distance, l_p, measured from the pivot points of the pendulum and of the inverted pendulum arms. The distance between the pivot points C_1 and C_2 is fixed and equal to l_d. All these hypotheses, are well satisfied in all our mechanical implementations of monolithic FP sensors.

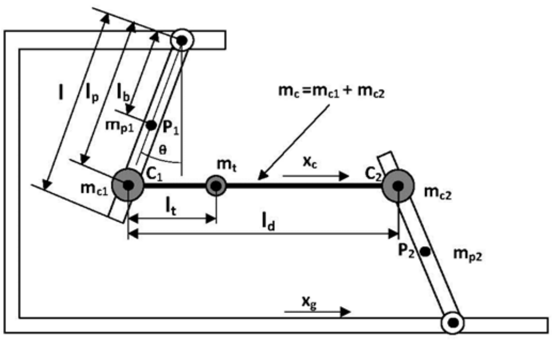

Figure 2.1. Folded Pendulum Mechanical Scheme.

Then, applying the simplified Lagrangian model developed by Liu, et al. (1997) for small deflection angles, θ, and integrating it with a dissipation term, for a better description of the FP performances (Acernese, et al., 2010b), were able to describe the basic FP dynamics, main characteristics and expected performances. It is, nevertheless important to underline here that design and implementation of optimized high performance FP sensors require a more detailed analysis of the FP dynamics, that can be obtained only with simulations based on very accurate numerical models, like the one we developed for this specific task (Acernese, et al., 2008), and that we are continuously improving and updating. According to this model, for small deflection angles, θ, the FP resonance frequency, f_o, is

$$f_o = \frac{\omega_o}{2\pi} = \frac{1}{2\pi}\sqrt{\frac{K_{g_{eq}} + K_{e_{eq}}}{M_{eq}}} = \sqrt{\frac{K_{eq}}{M_{eq}}} \tag{2.1}$$

where $K_{g_{eq}}$, the equivalent gravitational linear stiffness constant, and $K_{e_{eq}}$, the equivalent elastic constant, are defined, respectively, as

$$K_{g_{eq}} = (m_{p_1} - m_{p_2})\frac{gl}{l_p^2} + (m_{c_1} - m_{c_2})\frac{g}{l_p} \qquad K_{e_{eq}} = \frac{k_\theta}{l_p^2} \tag{2.2}$$

while M_{eq}, the equivalent mass, is defined as,

$$M_{eq} = (m_{p_1} + m_{p_2})\frac{l^2}{3l_p^2} + (m_{c_1} + m_{c_2})\frac{g}{l_p} \tag{2.3}$$

Eqn. 2.1 is the classic expression of the resonance frequency of a spring-mass oscillator with an equivalent elastic constant K_{eq} and mass M_{eq}. Note that with a suitable mechanical design of the FP mechanical components, the equivalent gravitational linear stiffness constant, $K_{g_{eq}}$, can assume negative values, partially compensating the equivalent elastic constant, $K_{e_{eq}}$, reducing the FP resonance. This means that a FP with a specific resonance frequency can be, relatively easily, obtained with a suitable design of its mechanical parts. Furthermore, the resonance frequency can be changed also on already implemented FP (e.g. FP optimization for a specific application), with a specially developed tuning procedure with a tuning mass, m_t, as explained in the following. It is important to underline that the sensitivity of a FP seismometer (open loop configuration) is strongly dependent on its resonance frequency, as it will be clarified in the following sections.

The addition of a tuning mass, m_t, positioned at a distance l_t from the pendulum-central-mass pivot point, C_1, as shown in Fig. 1, changes the values of the equivalent masses m_{c_1} and m_{c_2}, that are increased by fractions of the tuning mass, as function of its position, l_t, according to the relations

$$\Delta m_{c_1} = m_t\left(1 - \frac{l_t}{l_d}\right) \qquad \Delta m_{c_2} = m_t\left(\frac{l_t}{l_d}\right) \tag{2.4}$$

The equivalent gravitational linear stiffness constant, $K_{g_{eq}}$, and the equivalent mass, M_{eq}, change accordingly,

$$\Delta K_{g_{eq}} = (\Delta m_{c_1} - \Delta m_{c_2})\frac{g}{l_p} = m_t\left(1 - \frac{2l_t}{l_d}\right) \qquad \Delta M_{eq} = m_t \tag{2.5}$$

According to the position of the tuning mass, this term assumes positive or negative values. Hence, the FP resonance frequency, f_o, increases or decreases, respectively. In Figure 2.2, a picture of f_o vs. value (m_t) and position (l_t) of the tuning mass for a typical monolithic sensor is shown.

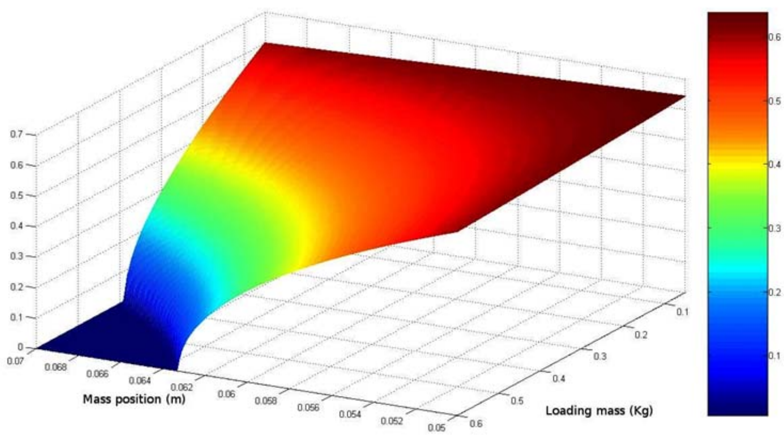

Figure 2.2. Resonance frequency, f_o, vs. tuning mass value, m_t, and its position, l_t, for a typical monolithic FP.

It is here worth underlining the importance of the FP tuning sensitivity for a comfortable and stable tuning, obtained deriving Eqn. 2.1 with respect to the position of the tuning mass, that is (Acernese, et al., 2010b).

$$S_{f_o} = \frac{df_o}{dl_t} = \frac{g}{2\pi l_d l_p} \frac{m_t}{\sqrt{M_{eq}(m_t) K_{eq}}} \tag{2.6}$$

As expected, Eqn. 2.6 demonstrates that the FP sensitivity is function of the value of the tuning mass, m_t, and that to obtain the same resonance frequency change, Δf_o, the heavier is the tuning mass, the smaller is its necessary displacement.

Defining, then, the coordinate of the FP frame (fixed to the ground) as x_g and the coordinate of the FP central mass (m_c) as x_c, then the mass displacement transfer function with respect to the ground displacement in the Laplace domain is (Acernese, et al., 2011)

$$H(s) = \frac{x_c(s) - x_g(s)}{x_g\,(s)} = \frac{-(1 - A_c)s^2}{s^2 + \frac{\omega_o}{Q(\omega_o)} s + \omega_o^2} \tag{2.7}$$

where $Q(\omega_o)$ is the global Quality Factor and

$$A_c = \frac{\left(\frac{l_p}{3l} - \frac{1}{2}\right)(m_{p_1} - m_{p_2})}{M_{eq}} \tag{2.8}$$

is the parameter related to the centre of percussion effects (Liu, Li and Blair, 1997). Eqn. 2.7 can then be rewritten in the Fourier domain as

$$H(\omega) = \frac{x_c(\omega) - x_g(\omega)}{x_g\,(\omega)} = \frac{(1 - A_c)\omega^2}{-\omega^2 + \frac{\omega_o}{Q(\omega_o)} j\omega + \omega_o^2} \tag{2.9}$$

The dependence of $Q(\omega_o)$ on the FP resonance angular frequency, ω_o, has been experimentally demonstrated and will be discussed in the following section.

Finally, it is important to underline here that the FP configuration couples horizontal forces and frame tilts. This is still an open problem, only partly solved, for example, if they are separate in band or if the FP is coupled with a tiltmeter of comparable sensitivity (Fan, et al., 1999; Wu, Fan and Luo, 2002; Bertolini, DeSalvo, Fidecaro and Takamori, 2006; Takamori, et al., 2011).

3. THE UNISA HORIZONTAL SEISMOMETER

The UNISA Horizontal Seismometer is a new FP implementation, developed starting from the FP original architecture (Fergusson, 1962) and from the monolithic design by Bertolini et al. (2006), that allows very compact and robust FP implementations. Actually, the use of circular hinges in this monolithic FP design puts a heavy constraint on the joint rotational angles, largely limiting its whole dynamics (few hundreds of microns). Therefore, the force feed-back configuration (accelerometer) was an obliged choice, with limitations in band and sensitivity due to the control electronic noise. We solved this problem enlarging the gaps among the arms, the central mass and the frame, increasing the sensor dynamics to few mm, but, as drawback, we were obliged to use elliptically shaped flexures, as suggested in (Bertolini, et al., 2006) and experimentally tested in (Acernese, et al., 2008). Although the instantaneous rotation centre is better defined with circular hinges (compared to the elliptical ones), a suitable choice of the hinge ellipticity factor in connection with the mechanical dynamics minimizes all the coupling effects. Moreover, they have the advantage both of a stiffness scaling down as $1/e$ (e is the ratio of the major to minor axes) (Smith, Badami, Dale and Xu, 1997), of a reduced stress and of a strain distributed over a larger length (Tseytlin, 2002).

We, then, designed and implemented very compact broadband single-axis monolithic FP horizontal sensors of reasonable size with very low natural resonance frequencies (down to ≈ 66 mHz) to be used both as seismometers (open loop configuration) and accelerometers (closed loop with an external force feed-back control systems). Furthermore the innovative application of laser optics techniques for the implementation of the FP monolithic readout (laser optical levers and laser interferometers), has improved its sensitivity, especially in the low frequency band, increasing, at the same time, its immunity to environmental noises (Acernese, et al., 2008). It is important to underline here that the sensitivity of the interferometric optical readout depends on many parameters, like the optical configuration, the quality of the laser, the open loop error signal extraction techniques used, etc.. Many configurations and techniques exist in literature suitable for this purpose, and applied to seismic sensors since long time, so that any improvement of the optical readout may be simply a matter of suitable choice and cost, and does not require special dedicated studies.

Actually, the main problem that prevented the use of monolithic FP as seismometers (open loop configuration) was geometric. In fact, all the previous versions of FP were designed with the constraint that the four joints, necessary for the mechanical implementation, work in tension. This technical choice led to the implementation of FP with asymmetric arms. In particular, the moment of inertia of the inverted pendulum arm cannot be minimized, becoming a real problem for the quality of the FP dynamics. These asymmetries become very relevant in the open loop configuration FP sensor. In fact, being the rotation centre of the elliptic hinges time and position dependent, the coupling of the inverted pendulum arm motion with the central mass motion largely increases the couplings of different degrees of freedom, reducing the quality factor and increasing the noise on the horizontal axis.

This problem was solved in the UNISA Horizontal Seismometer (Barone and Giordano, 2011), characterized by a symmetric FP configuration, that allows the optimization of the moments of inertia of both the arms according to the specific application. In this new design, the two joints of the inverted pendulum work in compression. In order to compare the results obtained with the UNISA Horizontal Seismometer and the previous monolithic FP versions we implemented this new Seismometer using the same material (Aluminium Alloy 7075-T6), the same dimensions $(134\,mm \times 134\,mm \times 40\,mm)$ and the same ellipticity (16/5) and thickness $100\,\mu m$ of the hinges of the previous versions. In Fig. 3.1 the UNISA Horizontal Seismometer is shown.

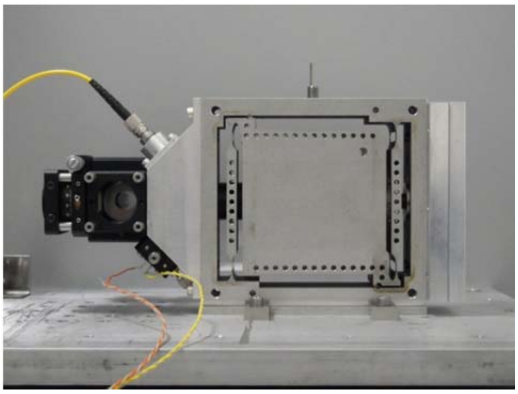

Figure 3.1. The UNISA Horizontal Seismometer.

Therefore, a sensor with no feed-back control system has the great advantage that there are no limitations to the band and sensitivity introduced by the control electronics, so that the quality of the instrument mainly depends on a careful and optimized mechanical design. The real limitations to the performances of a mechanical monolithic sensor become then the thermal noise, the sensitivity to the external temperature and acoustic noise (in air) and the readout sensitivity. Being the latter actually a laser optical readout (optical lever and laser interferometer), its quality is a problem of cost and portability of the sensor. In particular the monolithic horizontal FP sensor can be used both as stand-alone large-band high-dynamics seismometer/accelerometer for earthquake monitoring, for seismic noise monitoring for geophysics applications, for monitoring and control of civil and industrial buildings (dams, buildings, etc.) and as seismometer/accelerometer for the automatic control of mechanical multi/stage suspensions and inertial platforms (Acernese, et al.,2012b).

4. PRESENT PERFORMANCES THE UNISA HORIZONTAL SEISMOMETER

The performances of the UNISA Horizontal Seismometer were checked through a series of tests aimed both to demonstrate that the prototype follows the predictions of the theoretical/numerical models developed for simulation and design. Their reliability was proved by comparing the experimental monolithic FP transfer function at its natural design resonance frequency (Acernese, et al., 2008), made using a standard measurement procedure used in control theory to obtain the transfer function of a linear system injecting white noise, and checking the effective quality of the tuning procedure developed: a resonance frequency of $66\ mHz$ has been obtained. This result is still more relevant if the small dimensions of the monolithic FP are taken into account. It is anyway important to underline that tuning the FP at its lowest possible natural resonance frequency improves the sensor measurement band at low frequencies, but at the same time reduces the restoring force of the pendulum to external perturbations, increasing the probability for the test mass to touch the frame, saturating the sensor output. Although this may be again only a problem of dynamics for the UNISA Horizontal Seismometer (that can be partially solved enlarging the gaps among the central mass-arms and arms-frame), it is not at all a problem if it is configured as accelerometer, being the central mass always forced in its rest position by the force feed-back control.

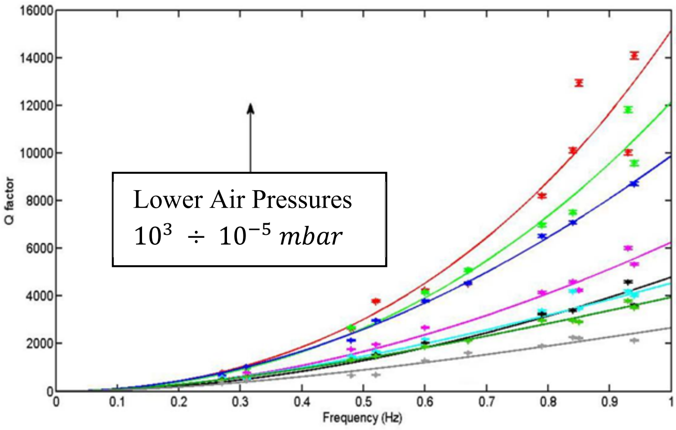

Figure 4.1. Quality Factor vs. Resonance Frequency for the UNISA Horizontal Seismometer.

The real problem is that the FP quality factor, Q, like every mechanical oscillator, decreases together with its natural frequency, so that the FP performances decrease moving its resonance frequency towards the low frequencies region. This effect is fully taken into account in Eqn. 2.7, where the theoretical prediction and/or the experimental measurements of the function $Q = Q(\omega)$ of the mechanical system become relevant. We remind that this function depends also on the value of the tuning mass, m_t. This dependence is function of the ratio m_t/m_c: the larger is this ratio, the larger is the increase of Q. In order to validate the UNISA Horizontal Seismometer we performed a series of tests to experimentally evaluate the function $Q = Q(\omega)$. We made all the tests positioning the sensor in a vacuum chamber and measuring the function $Q = Q(\omega)$ for different values of the pressure in the chamber and a $m_t = 240\ g$ tuning mass. We repeated the measures for different values of the resonance frequency, using the calibration procedure. The results are reported in Fig. 4.1. As expected, the Quality Factor increases at the increase of the resonance frequency and shows the expected parabolic dependence, $Q(f_o) = a \cdot f_o^2$ (the value of a depending on the air pressure). In particular, Fig. 4.1 shows that already at the atmospheric pressure and at the prototype design natural resonance frequency ($f_o \approx 0.721\ Hz$) the value of the quality factor is $Q > 1800$, thus demonstrating that the UNISA sensor perfectly fits for applications in air. Moreover, a quality Factor, $Q \approx 6000$ was measured for the prototype at the design natural resonance frequency with a moderate vacuum ($p = 10^{-5}\ mbar$), reaching values up to $Q \approx 14000$ for a natural resonance frequency of $f_o = 0.94\ Hz$. In synthesis, the sensor works very well both in vacuum and in air (the main goal of the FP monolithic new design). It is again relevant to underline that for this monolithic Aluminium (7075-T6) prototype values of $Q > 100$ are measured also for resonance frequencies below $100\ mHz$.

Finally, in Fig. 4.2 the best theoretical and experimental sensitivities curves are shown at ($T = 300$, assuming the FP tuned at a resonance frequency ($f_o = 100\ mHz$). The measurements were made with the FP central mass clamped to the frame, in air and with no thermal stabilization both for the optical lever (with PSD photodiodes) and for the interferometric readouts. The sensitivity of the STS-2 by Streckeisen (Nakayana, et al., 2004) and the Trillium-240 by Nanometrics (Nanometrics), representing the state-of-art of the low frequency seismic sensors are reported for comparison in this figure, together with the Peterson New Low Noise Model (NLNM) (Peterson, 1993) and the McManara and Bouland Noise Model (McManara and Buland, 2004), representing the minimum measured Earth noise evaluated from a collection of seismic data from several sites located around the world: noise levels below this are never - or extremely rarely - observed. We just recall here, as pointed in a previous section, that many configurations and techniques exist in literature suitable for this the monolithic FP optical readout, may be simply a matter of suitable choice, taking into account parameters like robustness, compactness, cost, and does not require special dedicated studies.

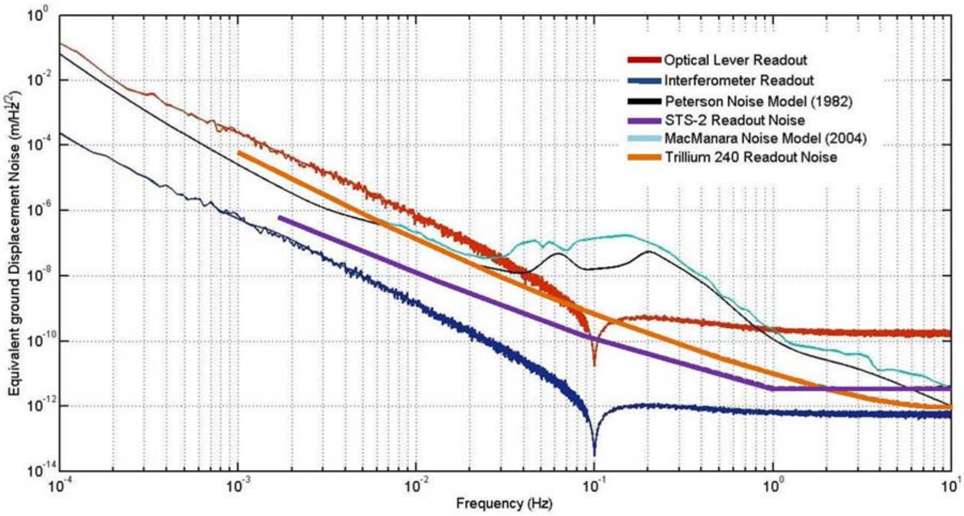

Figure 4.2. Measured readout sensitivity curves of the UNISA Horizontal Seismometer, compared with the Peterson Low Noise Model, with the McManara Noise Model and with two commercial sensors: STS-2 by Streckeisen and Trillium-240 by Nanometrics.

5. EXPERIMENTAL RESULTS OF THE SEISMIC STATION AT LNGS

The seismic station at the LNGS was built in 2010 on a concrete platform located on the bedrock. In August 2011, after the installation of the two new UNISA Horizontal Seismometers, the seismic station become equipped with:
- two accelerometers "Episensor" ES-T by Kinemetrics;
- two parallel monolithic FP Seismometers (Acernese, et al., 2008) with laser optical lever readout;
- two parallel UNISA Horizontal Seismometers with laser optical lever readout;
- two environmental monitoring boxes, equipped with temperature pressure and humidity sensors.

The environmental conditions within the seismic station are very stable. The seismic station guarantees the thermal stability of the sensors. In fact, although the environmental temperature outside the whole station changes at most of 2^oC along the year, no correlation effects between temperature changes and FP output have been highlighted. The data-acquisition system includes the configuration of the local network and remote access to PCs. The acquisition system is based on the PCI 6289 card from National Instruments, based on a 18 bit ADC and an internal amplifier with a maximum amplification of 100. The input range is limited to $\pm 10\ V$. The Data Acquisition is managed by Labview programs generating analog outputs, very useful to simplify the installation procedure of the seismometer. The data are first stored in ASCII files as $3600\ s$ records sampled at $20\ kHz$ and, then, down sampled at $200\ Hz$.

To test the sensors capability to measure seismic signal we have analyzed about eight months of data downsampled at $2\ kHz$, taken in the INFN Gran Sasso National Laboratory since August 2011. The first analysis was aimed to understand the sensor frequency bands characterized by enough sensitivity for seismic signal measurement with a good signal-to-noise ratio. For this task, we evaluated the square spectral coherence, γ^2, calculated using the output two FP UNISA Seismometers positioned on the same basement in parallel configuration. The γ^2 spectral density, compared to a threshold value of 0.95 confidence interval, as illustrated by Miles (Miles, 2011) is shown in Fig. 5.1.

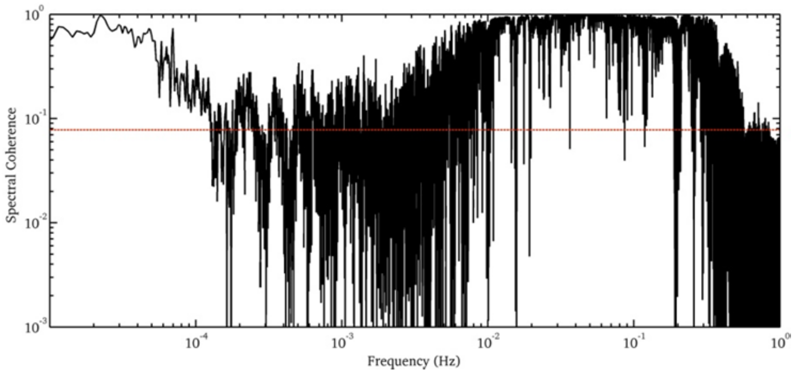

Figure 5.1: Spectral Coherence

As it can be seen in Fig. 5.1, the UNISA FP Horizontal Seismometer shows a variable coherence spectral density, although almost above threshold. In particular, in the teleseismic earthquake frequency band ($1\ mHz\ \div 1\ Hz$) and in the Earth tides frequency band ($0.05\ mHz$) the coherence is near the unit value. This means that the sensor can measure very far big earthquakes with high SNR. This sensor characteristic is show in Fig. 5.2, where, for example, a couple of earthquakes is shown (M8,6–Sumatra–April 11, 2012, 08:38:37 UTC and M8,2–Sumatra–April 11, 2012, 10:43:09 UTC).

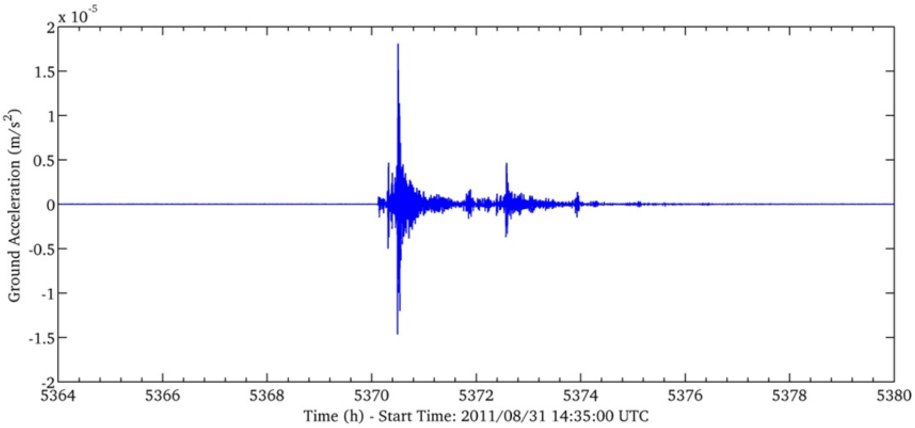

Figure 5.2. Recorded Earthquakes: (M8,6 – Sumatra – April 11, 2012, 08:38:37 UTC and M8,2 – Sumatra – April 11, 2012, 10:43:09 UTC).

Furthermore, Fig. 4.2 and Fig. 5.1 shows that also the Earth Tides can be useful measured with good SNR. Fig. 5.3 show the power spectral density of Earth Tides as measured by FP Seismometers. This figure also shows the theoretical frequency values of Earth tides (triangles). It is easy to recognize the semi-diurnal tidal triplet (M2,S2,N2) and some of diurnal tidal constituents (K1, O1,P1). Moreover, several components are present in the period band $T < 24\ h$ that have to be identified.

Another very interesting seismic frequency band is the $0.1\ \div 10\ mHz$ one, where there are the Earth normal resonant modes. From analysis of coherence and of the readout noise, it is possible to affirm that at the state of art the UNISA Horizontal Seismometer is enough sensitive to measure Earth Normal Modes, but with low SNR, so that it is necessary a long set of data and several big earthquakes to excite them. The installation of the interferometric readout improves sensitivity and SNR.

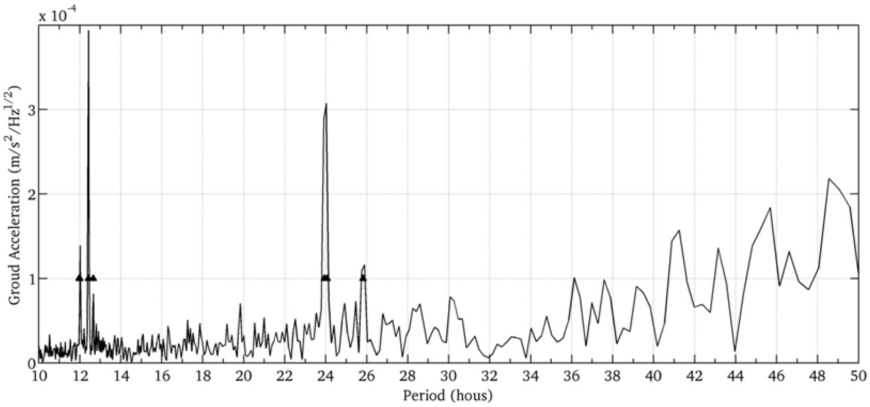

Figure 5.3 Power Spectral Density of Earth Tides.

Finally, Fig. 5.4 shows low seismic noise as measured under the INFN Gran Sasso National Laboratory (LNGS) in the microseismic frequency band. As it can be seen, the FP sensor has enough sensitivity to resolve also the two microseismic peaks ($0.2\ Hz\ \div 0.3\ Hz$), despite they are very close to low noise Peterson Model, as in the LNGS.

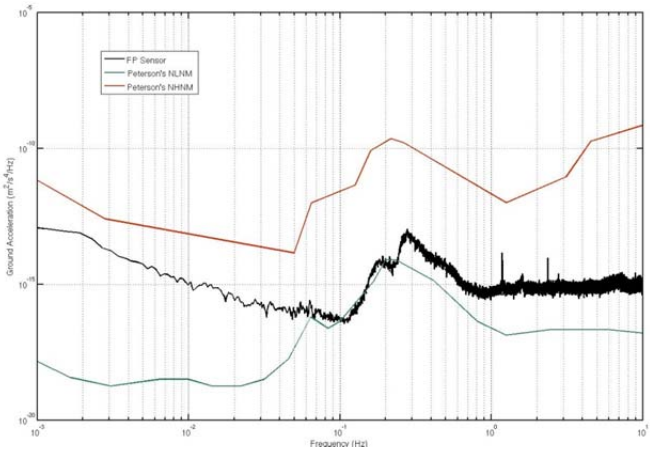

Figure 5.4. Power Spectral Density of ground acceleration (compared with Peterson's New Noise Model.

In conclusion, after the evaluation of the sensor performances and analysis of the recorded data in different frequency bands, we can affirm that the measurement band of the present implemented version of the UNISA Horizontal Seismometer with a laser optical lever readout is at least eight decades, $0.1\ \mu Hz\ \div 10\ Hz$.

The experimental results obtained and the analysis of the measurements at the INFN Gran Sasso National Laboratory (LNGS) show that the sensor in the present configuration is fully ready and qualified for experimental applications. In the next months it is scheduled the installation of a network of these sensors for the long term characterization of the Sos Enattos mine (Lula, Sardinia, Italy), one of the candidates sites in Europe for the installation of the Einstein Telescope (ET) (Punturo, et al., 2010), an interferometric detector of gravitational waves of the new generation.

Of course, the results presented in the paper show that the present version of the FP monolithic sensor has not yet reached its ultimate sensitivity. For example, the change of the optical lever readout module (used at LNGS) with the laser interferometric readout module (fully tested and qualified), improves its sensitivity of at least two orders of magnitude along all the measurement band, as shown in Figure 4.2. Further improvements of sensitivity and band aimed to optimize the mechanical and optical components are under study and/or test.

AKCNOWLEDGEMENT
We acknowledge the Director of the INFN Laboratori Nazionali del Gran Sasso, Prof. Lucia Votano. We acknowledge Ing. Aprili and Ing. Gallese for their helpful technical support.

REFERENCES

Acernese, F., De Rosa, R., Giordano, G., Romano, R. and Barone, F., 2008. Mechanical monolithic horizontal sensor for low frequency seismic noise measurement. *Rev. Sci. Instrum.* **79**, 074501.

Acernese, F., Giordano, G., Romano, R., De Rosa, R. and Barone, F., 2010a. Tunable mechanical monolithic sensor with interferometric readout for low frequency seismic noise measurement. *Nucl. Instrum. and Meth. A* **617**, 457-458.

Acernese, F., De Rosa, R., Garufi, F., Giordano, G., Romano, R., and Barone, F., 2010b. Tunable mechanical monolithic horizontal sensor with high Q for low frequency seismic noise measurement. *Journ. of Phys. Conf. Series* **228**, p.0120351.

Acernese, F., De Rosa, R., Giordano, G., Romano, R., Vilasi, S., Barone, F., 2011. Low Frequency - High Sensitive Tunable Mechanical Monolithic Horizontal Sensors. *SPIE Intern. Conf. on Sensors and Smart Structures Technologies for Civil, Mechanical, and Aerospace Systems 2011*.**7981**: 79814J-1-79814J-11.

Acernese, F., De Rosa, R., Giordano, G., Romano, R., Vilasi, S., and Barone, F., 2012a. Low frequency/high sensitivity horizontal monolithic sensor. *SPIE Intern. Conf. on Sensors and Smart Structures Technologies for Civil, Mechanical, and Aerospace Systems 2012a*. **8345:** 83453D-1, 83453D-9.

Acernese, F., De Rosa, R., Giordano, G., Romano, R., Vilasi, S., and Barone, F., 2012b. A new control approach for the design and implementation of low frequency large band mechanical suspensions and inertial platforms. *SPIE Intern. Conf. on Sensors and Smart Structures Technologies for Civil, Mechanical, and Aerospace Systems 2012b*. **8345**: 83453C-1-83453C-6.

Barone, F., Giordano, G. (2011). Low frequency folded pendulum with high mechanical quality factor, and seismic sensor utilizing such a folded pendulum. *International application published under the patent cooperation treaty (PCT).* **WO 2011/004413 A3**.

Bertolini, A., DeSalvo, R., Fidecaro, F., Francesconi, M., Marka, S., Sannibale, V., Simonetti, D., Takamori, A. and Tariq, H., 2006. Mechanical design of a single-axis monolithic accelerometer for advanced seismic attenuation systems. *Nucl. Instr. and Meth. A* **556**, 616-623.

Bertolini, A., DeSalvo, R., Fidecaro, F. and Takamori, A., 2006. Monolithic Folded Pendulum Accelerometers for Seismic Monitoring and Active Isolation Systems. *IEEE Trans. on Geosci. And Rem. Sens.* **44**, 273-276.

Fan, S., Cai Y., Wu S., and Luo, J., and Hsu, H., 1999. Response of a folded pendulum to tilt tides. *Physics Letters A* **256,** 132–140.

Fergusson, E.S., 1962. *US Nat. Museum Bull.* **228**, 185.

Liu, J., Li, J. and Blair, D.G., 1997. Vibration isolation performance of an ultra-low frequency folded pendulum resonator. *Phys. Lett. A* **228**, 243-249.

Liu, J., Blair, D.G. and Li, J., 2004. Near-shore ocean wave measurement using a very low frequency folded pendulum. *Meas. Sci. Technol.* **9**, 1772-1776.

McManara D.E. and Buland, R.P., 2004. Ambient Noise Levels in the Continental United States. *Bull. Seism. Soc. Am.* **94**, 1517-1527.

Miles, J.H., 2011. Estimation of signal coherence threshold and concealed spectral lines applied to detection of turbofan engine combustion noise. *J. Acoust. Soc. Am.* **129**, 3068-3081.

Nakayama, Y., et al. (2004) Performances test of STS-2 seismometers with various data loggers. *IWAA2004*, CERN, Geneva, 4-7 October 2004 (2004).

Nanometrics: http://www.nanometrics.ca/products/trillium-240.

Peterson, J., 1993. Observations and modelling of background seismic noise. *Open-file report 93-322, U. S. Geological Survey,* Albuquerque, New Mexico.

Smith, T.S., Badami, V.G., Dale, J. S., Xu Y., 1997. Elliptical flexure hinges. *Rev. Sci. Instrum.* **68**, 1474-1484.

Takamori, A., Bertolini, A., DeSalvo, R., Araya, A., Kanazawa, T., and Shinohara, M., 2011. Novel compact tiltmeter for ocean bottom and other frontier observations**.** *Meas. Sci. Technol.* **22**, 115901.

Tseytlin, M.Y., 2002. Notch flexure hinges: An effective theory. *Rev. Sci. Instrument* **73**, p.3363.

Zhou, Z.B., Yi Y.Y., Wu, S.C. and Luo, J., 2004. Low-frequency seismic spectrum measured by a laser interferometer combined with a low-frequency folded pendulum. *Meas. Sci. Technol.* **15**, 165-169.

Wu, S., Fan, S., and Luo, J., 2002. Folded pendulum tiltmeter. *Rev. Sci. Instrum.* 73, 2150-2156.

Punturo M., et al., ET Science Team, 2010. The Einstein Telescope: a third-generation gravitational wave observatory. *Class. Quantum Grav.* 27, 194002.